

## Rapid Prototyping of Nanostructured Materials with a Focused Ion Beam

Oliver WILHELMI, Steve REYNTJENS, Christoph MITTERBAUER, Laurent ROUSSEL,  
Debbie J. STOKES, and Dominique H. W. HUBERT

FEI Company, Building AAE, P.O. Box 80066, 5600 Eindhoven, The Netherlands

(Received November 8, 2007; accepted February 5, 2008; published online June 20, 2008)

State-of-the-art focused ion beam (FIB) technology combined with high-performance scanning electron microscopy (SEM) is making a big impact on nanotechnology, particularly with the ability to use either focused ions or electrons to perform advanced nanolithography. Achieving the highest standards requires an understanding of the physics and chemistry of the system as a whole, which contains ions and electrons of various energies and origins, substrates with a range of electrical and mechanical properties, and reactive gases capable of specific effects on sputtering and re-deposition. We have built up a detailed knowledge of these complex parameters and, accordingly, have developed new strategies, allowing us to generate high resolution nanolithographic structures down to a few nanometers. We compare and contrast different strategies in order to demonstrate the importance of factors such as single- or multi-pass execution as well as milling order and time-dependent considerations. [DOI: [10.1143/JJAP.47.5010](https://doi.org/10.1143/JJAP.47.5010)]

KEYWORDS: nanofabrication, nano-prototyping, DualBeam, FIB SEM

### 1. Introduction

Focused ion beam (FIB) milling of patterns in any kind of material and the precise beam induced deposition of various materials, in one single instrument, are recognized as novel ways of carrying out true, rapid prototyping. The capability to observe the patterning process live and to immediately image the resulting structures with a high-resolution scanning electron microscope (SEM) in the same instrument (see, for example, Fig. 1) offers unique control over the process. Pattern modifications can be carried out instantaneously and prototype functionality can be tested before the final layout of a device is established for batch fabrication. Beam induced deposition of different materials can be combined with FIB milling without the need of several aligned lithography steps; stacks of dissimilar materials can be structured in one single milling process; patterns can be added to existing structures on a substrate (e.g., on nanoimprint stamps). Patterned substrates are immediately available for further processing or characterization. Once a prototype has been tested successfully, batch nanofabrication processes can be integrated with electron beam lithography using the SEM column of the instrument. The capability to pattern almost any material and fabricate layers composed of dissimilar materials makes the FIB highly versatile.<sup>1–3)</sup> The ability to rapidly prototype and perform resist patterning for nanofabrication in one instrument holds the potential to deliver much faster proof-of-concept results for devices and point the way towards volume manufacturing.

### 2. Ion Beam Nanoprototyping

Pattern generators that are used for electron beam resist exposure can also be used for direct FIB patterning. The apparent similarities in controlling and steering the beam often lead researchers to carry forward electron beam lithography exposure strategies as a technique for FIB pattern execution. This, however, neglects fundamental differences, such as exposure to certain doses before resist development in electron beam lithography against the instantaneous removal or deposition of material with a FIB.<sup>4,5)</sup> The following sections illustrate the significance of adequate pattern execution for successful FIB patterning.

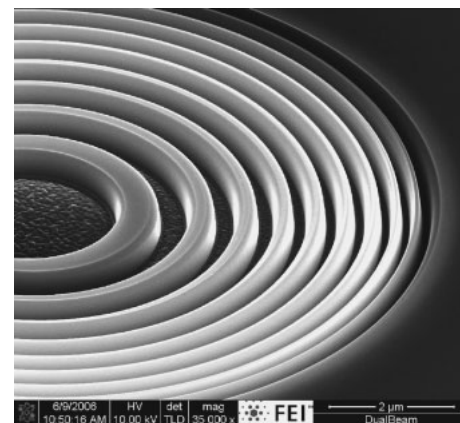


Fig. 1. Fresnel zone plate milled into silicon using a beam of focused gallium ions, demonstrating excellent side wall quality and high aspect ratio.

#### 2.1 Milling strategies for the accurate control of dimensions

The profile of a single point milled into any substrate will partly be determined by the profile of the FIB itself. On the other hand, since the FIB immediately sputters away substrate material, a void forms while the FIB continues milling at the same position. Consequently, ions hit the sloped sidewalls of the forming void, especially at longer pixel dwell times. As sputter yields depend on the angle of the incident ions, milling rates depend on pixel dwell time. Another aspect that needs to be taken into consideration is the re-deposition of sputtered material that will occur inside the milled structures.

For illustrative purposes a Y-junction of 100 nm wide trenches, 200 nm deep, was milled into silicon. Based on ion beam current, accelerating voltage and substrate material, a pitch of 8.5 nm was calculated and automatically set in order to have a 50% overlap of adjacent mill points. The trenches were patterned in a serpentine sweep. Figure 2(a) shows the resulting pattern when all individual pattern elements are milled in parallel and with multiple passes of the FIB as per

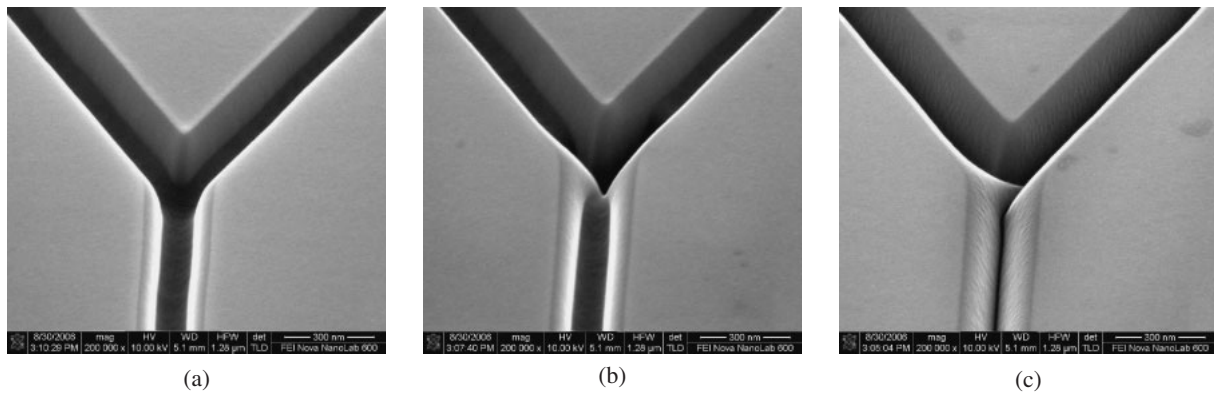


Fig. 2. (a) Parallel multi-pass milling, (b) serial multi-pass milling, and (c) single-pass milling, adopting an electron beam lithography strategy. All trenches are 100 nm wide and 200 nm deep.

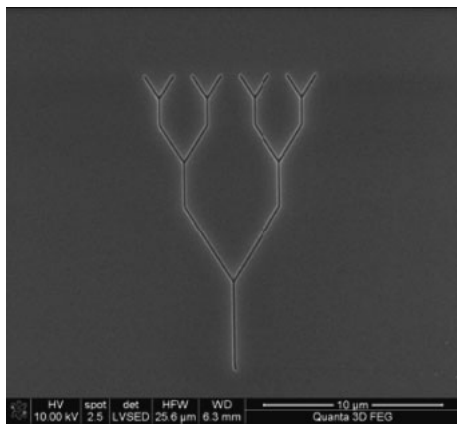


Fig. 3. The nanofluidic trench pattern milled into quartz using drift suppression. All trenches are 100 nm wide.

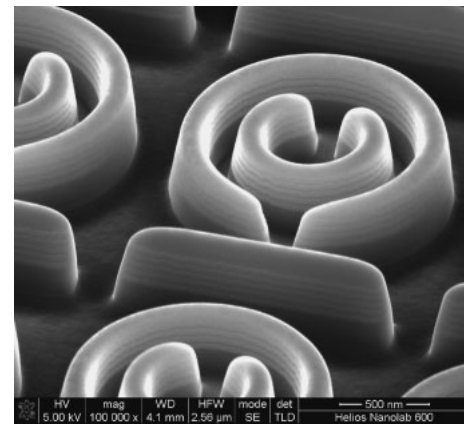


Fig. 4. A split ring resonator pattern in a  $\text{SiO}_2$  layer with a Ge multi quantum well. The width of the rings and the trench in between is 120 nm, the pattern depth is 800 nm.

default conditions, in this case 1  $\mu\text{s}$  dwell time, 882 passes. Figure 2(b) shows the same pattern milled with multiple passes as in Fig. 2(a), but this time serially: milling the legs of the Y-junction one after the other. Figure 2(c) shows the resulting pattern when the entire FIB dose is delivered in one single pass, in this case with 882  $\mu\text{s}$  dwell time, as it is done when an electron beam lithography pattern generator is used to steer the FIB.

The parallel multi-pass milling of Fig. 2(a) results in a trench pattern that could directly be used in a fluidic device for instance. The serial multi-pass milling in Fig. 2(b) leads to artifacts at the junction, while the single-pass milling in Fig. 2(c) shows evident re-deposition on the sidewalls leading to a V-shaped line profile and, again, artifacts at the junction. The short pixel dwell times in multi-pass milling avoid the formation of strong topography in one pass, thus yielding homogeneous pattern depth. This pass is repeated until the target depth is reached. The milling of the entire pattern until completion prevents the build-up of re-deposition. In contrast, a single-pass pattern exhibit pronounced milling artifacts which reflect the direction of the sweeps and the leading edge.

Parallel multi-pass milling as adequate patterning strategy for ion beam nanoprotyping applies to any pattern geometry and substrate material. Figure 3 shows the complete trench pattern of Fig. 2, this time milled into

quartz. Milling into quartz is more demanding due to the accumulation of positive charge during ion beam irradiation and the formation of a positive surface potential as a result of secondary electron emission. We have developed a method for suppressing ion beam drift using a defocused, site specific, low energy primary electron beam, and have derived an analytical method to correlate the ion and electron beam energies and currents with other parameters required for electrically stabilizing these materials,<sup>3)</sup> enabling us to create high resolution nanostructures even in electrically insulating substrates. Yet another example is presented in Fig. 4, showing details of a split ring resonator array which was milled into a layer of  $\text{SiO}_2$  with a Ge multi quantum well.

## 2.2 Material properties of nanostructures

The Ge quantum well in the  $\text{SiO}_2$  layer in Fig. 4 is clearly visible in the pattern side walls, indicating that the material properties of elaborate material systems are maintained during ion beam nanoprotyping. In order to qualify the impact of FIB milling on substrate materials in greater detail, a cross-sectional transmission electron microscope (TEM) sample was prepared and investigated in a TEM. The surface of the pattern sidewalls in Fig. 5(a) shows a 20-nm layer in which the implantation of Ga ions into the substrate material is visible. Ion implantation and amorphization

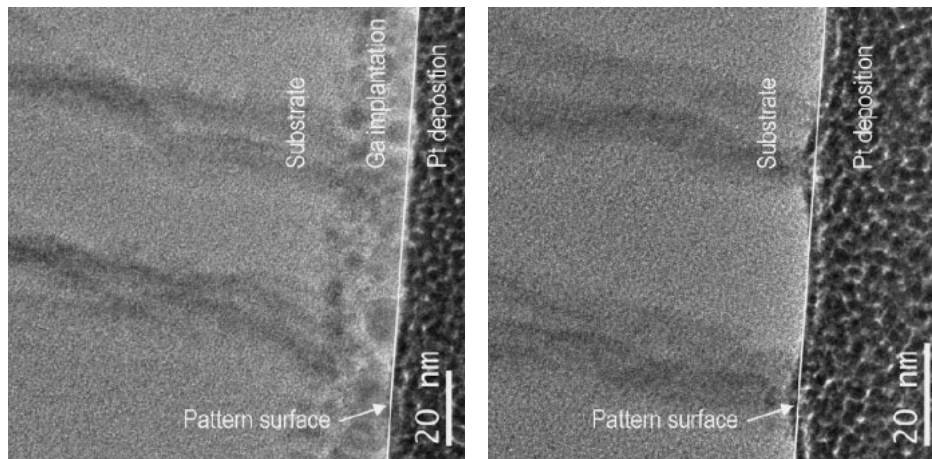


Fig. 5. Cross-sectional TEM images of the pattern sidewalls. The dark spots on the right hand side result from Pt deposition in the TEM sample preparation process and are not part of the pattern surface. The Ge quantum wells are well visible in the  $\text{SiO}_2$ . (a) Pattern sidewall milled with a 30-kV FIB. The darker patches at the pattern surface result from the implanted Ga. (b) Pattern sidewall milled with a 5-kV FIB. No Ga implantation is visible along the pattern surface.

in FIB milled Si surfaces are well documented for the preparation of TEM samples where focused Ga ion beams with low accelerating voltages are routinely used for minimizing the Ga implantation into high quality TEM samples.<sup>6)</sup> In an attempt to apply these techniques to FIB nanoprototyping, a trench was milled into the same substrate with a 5-kV FIB. Figure 5(b) shows cross-sectional TEM images of the side walls, this time without any visible Ga implantation.

A low-kV FIB is obviously favorable for nanoprototyping in terms of material properties; however a low-kV FIB does impose restrictions on the achievable prototypes: the FIB current is decreasing with decreasing accelerating voltage, leading to longer patterning times. Furthermore, the minimum achievable feature size as well as the maximum aspect ratio will be limited at lower accelerating voltages. The ideal conditions for any FIB nanoprototype will thus be a compromise of tight control of critical dimensions at the highest accelerating voltage and the least possible surface modification at low accelerating voltages, whereby awareness and understanding of surface modifications are the base for process optimization and successful FIB nanoprototypes.

As optical nanodevices are deemed potentially most sensitive to Ga implantation, an InP substrate was chosen for FIB milling of the same Fresnel zone plate pattern as in Fig. 1. Figure 6 shows the result achieved with a 30-kV FIB. The material that can be seen on the pattern sidewalls is attributed to differential milling, i.e. in this material system P is removed quicker than In due to its lower mass and lower surface binding energy, leaving excess In on the pattern surfaces.<sup>7,8)</sup> Figure 7(a) shows a cross-sectional TEM image of a pattern sidewall surface. The 35 nm wide damage layer on the pattern surface can clearly be distinguished from the crystalline InP bulk material. The pattern was then repeated with an 8-kV FIB resulting in a pattern surface as shown in Fig. 7(b), this time with a damage layer reduced to about 20 nm and less defined. The analytical results of the atomic Ga concentration in the InP sidewalls from EDX analysis is shown in Fig. 8. The 30-kV FIB pattern has a peak

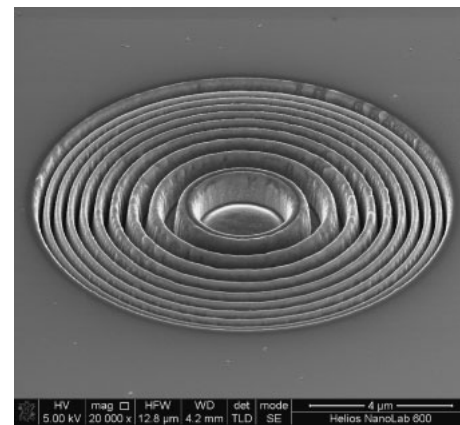


Fig. 6. High aspect ratio Fresnel zone plate milled into InP using a 30-kV FIB. The pattern surface shows the effect of the different sputter yields for In and P.

concentration of 20% Ga, while the 8-kV FIB pattern has a reduced peak concentration of 10%. In addition, the analytical results include those of a 30-kV FIB pattern with a 2-kV FIB cleaning of the entire pattern. It can be seen that about 20 nm of the damage layer could be removed; reducing the peak Ga-concentration to just over 10% and reducing the damage layer width to 20 nm as well, showing that proven techniques for TEM sample preparation can be applied to nanoprototyping as well.

### 3. Beam-Induced Chemical Vapor Deposition

In conjunction with a suitable gas delivery system, the FIB can be used to form localized, site-specific chemical vapor deposition of materials such as tungsten, platinum, gold, carbon and silicon oxide. It is therefore possible to create multi-layered devices in a variety of configurations. Figure 9(a) shows a plan view of such a FIB-assisted chemical vapour deposition (CVD) structure, while Fig. 9(b) shows a side view, after cross-sectioning with the FIB.

The properties of materials deposited by beam induced deposition can be substantially different to materials deposited by conventional nanofabrication techniques. The

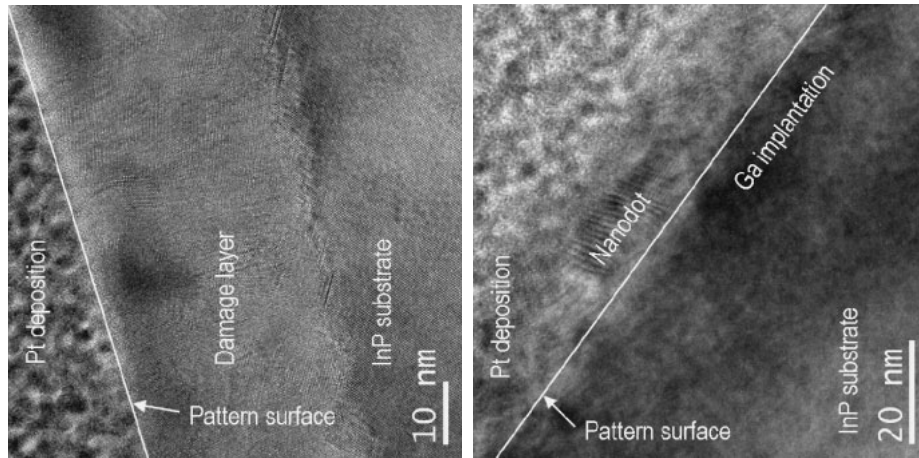


Fig. 7. Cross-sectional TEM images of the pattern sidewalls. The small spots on the left hand side result from Pt deposition in the TEM sample preparation process and are not part of the pattern surface. (a) Pattern sidewall milled with a 30-kV FIB. A 35 nm damage layer can clearly be distinguished from the InP substrate. (b) Pattern sidewall milled with an 8-kV FIB. The darker zone along the surface indicates the Ga implantation. The particle on the pattern surface with a distinct internal structure is one of the nanodots that have formed due to differential milling.

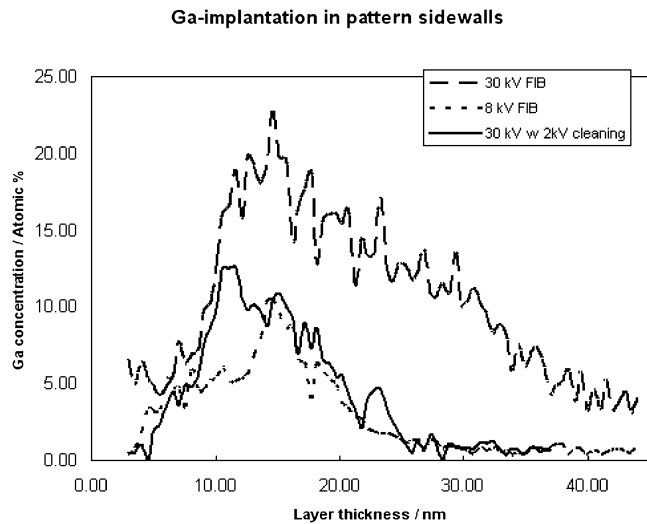
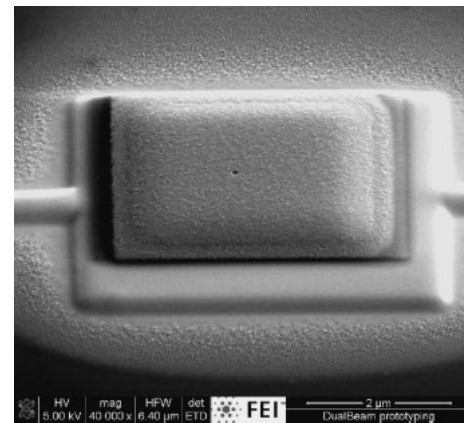


Fig. 8. Analytical results of the Ga implantation for different FIB settings. There is no accurate definition of the exact interface hence the different curves probably have a small horizontal offset. It is apparent that both, low-kV FIB milling and low-kV cleaning of 30-kV FIB patterns can be considered useful means for reducing Ga concentration and damage layer thickness.

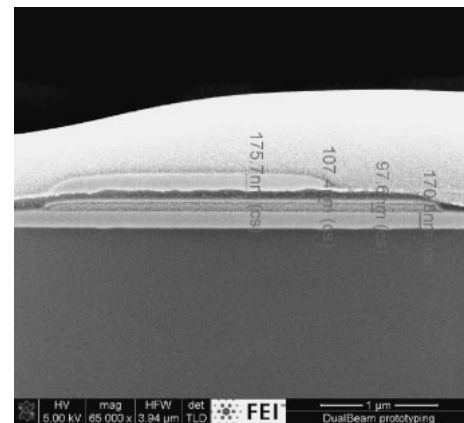
inclusion of molecules of the gaseous precursor can generate high contents of carbon in the deposits (deposits typically also include gallium from the ion beam). Although material properties may be different from the final device made by batch fabrication, FIB prototypes are well suited for electrical testing or catalytic functionality, for instance. Ultimately, FIB prototypes should be seen as a means to shorten development times in the initial and intermediate phase of a research project. Many critical process and application challenges can be tackled while a batch process is still under development.

**4. Conclusions**

A dedicated patterning strategy for rapid prototyping with the FIB has been shown to be of crucial importance for



(a)



(b)

Fig. 9. (a) Intermediate step of a cross-bar architecture intended for self-assembly of alkanethiol-based functional molecules. Bright square and contact lines: W-deposition; buried square: Au deposition; rough deposition on top: SiO<sub>2</sub> insulator deposition. As a last step, a 50 nm hole was milled through the SiO<sub>2</sub> insulator down to the Au layer to allow selective self-assembly inside the hole. (b) FIB cross-section through the cross-bar architecture of Fig. 3(a) after top-electrode deposition. The bright layer on top is a Pt deposition for facilitating FIB cross-sectioning. Clearly visible are: W top electrode (176 nm), the SiO<sub>x</sub> insulating layer (107 nm), Au layer (98 nm), and the W bottom electrode (171 nm).

successful FIB prototypes. The ability to observe the patterning process live with a high resolution SEM gives the operator immediate insight and direct control over the patterning process. In addition, a batch fabrication process can be developed with the electron column as patterning tool for electron beam lithography. The material properties of any FIB prototype need to be taken into account in the design of experiment and in the interpretation of results from application testing.

#### Acknowledgements

Our colleagues Tomas Vystavel and Marc Castagna are kindly acknowledged for their contribution in the prototyping results on quartz.

- 1) P. M. Nellen, V. Callegari, and R. Brönnimann: *Microelectron. Eng.* **83** (2006) 1805.
- 2) Y. Q. Fu, N. Kok, and A. Bryan: *Microelectron. Eng.* **54** (2000) 211.
- 3) D. J. Stokes, T. Vystavel, and F. Morrissey: *J. Phys. D* **40** (2007) 874.
- 4) B. I. Prenitzer, C. A. Urbanik-Shannon, L. A. Giannuzzi, S. R. Brown, R. B. Irwin, T. L. Shofner, and F. A. Stevie: *Microsc. Microanal.* **9** (2003) 216.
- 5) L. A. Giannuzzi, B. I. Prenitzer, and B. W. Kempshall: in *Introduction to Focused Ion Beams*, ed. L. A. Giannuzzi and F. A. Stevie (Springer, New York, 2005) p. 13.
- 6) L. A. Giannuzzi, R. Geurts, and J. Ringnalda: *Microsc. Microanal.* **11** (2005) Suppl., 828.
- 7) V. Callegari and P. Nellen: *Phys. Status Solidi A* **204** (2007) 1665.
- 8) V. Callegari, P. Nellen, U. Sennhauser, P. Strasser, and F. Robin: presented at 51st Int. Conf. Electron, Ion, Photon Beam Technology for Nanofabrication, Denver, CO, U.S.A., PL-5, 2007.